

# The effects of citric and acetic acids on the formation of calcium-deficient hydroxyapatite at 38 °C

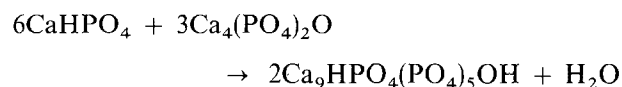
K. S. TENHUISEN, P. W. BROWN

*Department of Materials Science, University Park, PA 16802 USA*

This study is concerned with the formation of calcium-deficient hydroxyapatite at physiological temperature. Isothermal calorimetry, solution chemistry, scanning electron microscopy, BET surface area analyses and FTIR spectroscopy were used to characterize the kinetics of HAp formation and the microstructure of the HAp formed in varying concentrations of citric and acetic acids, and in deionized water. The kinetics of HAp formation are a strong function of both the concentration and type of acid. Acetic acid accelerates reaction due to pH effects. Citric acid retards HAp formation by citrate adsorption on the precursor and product phases. The results obtained indicate that hydroxyapatite formation can be tailored to address the requirements needed for eventual clinical applications.

## 1. Introduction

The ability to form hydroxyapatite (HAp) at physiological temperature is important if a biocompatible, bioresorbable bone substitute is to be developed. It has been demonstrated that HAp can be formed at low temperature by a cement-like reaction [1–4]. This occurs by an acid–base reaction involving tetracalcium phosphate ( $\text{Ca}_4(\text{PO}_4)_2\text{O}$  or TetCP) and an acidic calcium phosphate, such as monocalcium phosphate monohydrate ( $\text{Ca}(\text{H}_2\text{PO}_4)_2 \cdot \text{H}_2\text{O}$ ), anhydrous dicalcium phosphate ( $\text{CaHPO}_4$  or DCP), or dicalcium phosphate dihydrate ( $\text{CaHPO}_4 \cdot 2\text{H}_2\text{O}$  or DCPD). A typical reaction illustrating the formation of calcium deficient (Ca/P = 1.5) HAp is shown below:



HAp formed by this method has the advantage of setting and hardening at or below physiological temperature and in the presence of body fluids. It is thus a very attractive reaction for biocomposite applications.

The present investigation was performed to establish the effects of citric and acetic acids on the formation of calcium deficient HAp (Ca/P = 1.5) by the above reaction. Control of the kinetics of HAp formation and microstructure with which it forms are both important in tailoring a synthetic material to serve prosthetic functions. Citrate anion is present in bone mineral and is believed to play an important role in the formation and/or dissolution of bone apatite. As a consequence, the effects of citrate on the formation of various calcium phosphates, on their transformations, and on their solubilities has been studied [5–12]. It has been shown that citrates adsorb to the surfaces of HAp, octacalcium phosphate, and DCPD [5]. Holt *et al.* [13] found that citrates stabilized amorphous

calcium phosphate at pH values lower than those normally observed in solution precipitation reactions. This was attributed to the ability of citrate to inhibit the nucleation and growth of crystalline phases, namely HAp and DCPD. It has been proposed that the citrate molecule displaces surface phosphates in apatite [6,10]. However, the nature of the citrate/apatite interaction and manner in which citrate is present in apatite is still not well established. Therefore, the effects of citric acid on HAp formation was selected for study.

Molecular conformation and the number of carboxyl groups greatly influence adsorption/complexing properties with cations in solution and in solids [9, 14]. Therefore, acetic acid was chosen to compare the influence of a monoprotic acid on HAp formation to that of triprotic citric acid.

## 2. Experimental procedure

### 2.1. Precursor processing

TetCP was prepared by a solid-state reaction between commercially available reagent grade  $\text{CaHPO}_4$  and calcium carbonate at 1450 °C for 4 h. These were mixed in the proportion required to produce TetCP and milled before firing to obtain a homogeneous mixture. After firing, the TetCP was ground by hand and then milled to an average particle size of a few micrometres. Phase purity was confirmed by X-ray diffraction. An intimate mixture of the HAp precursors was achieved by milling TetCP with particulate DCP. X-ray diffraction verified the presence of these calcium phosphate reactants after milling.

### 2.2. X-ray diffraction, scanning electron microscopy, and surface area.

Powder X-ray analysis was performed on a Scintag

diffractometer using Cu K $\alpha$  radiation, a step size of 0.02 degrees, and a scan rate of 2 degrees per minute. A scan range between 20 and 35 degrees 2 $\theta$  was used when HAp was formed in deionized water and acetic acid. This range was extended to 4 and 35 degrees 2 $\theta$  for samples containing citrates because the most intense calcium citrate peak occurs between 4 and 10 degrees 2 $\theta$ . Microstructural development was observed using a conventional dual stage scanning electron microscope. The surface area of selected samples were obtained using the nitrogen BET method. Samples were dried at 120°C in a vacuum oven for 16 h and then at 170°C to remove surface water prior to nitrogen adsorption.

### 2.3. Reaction kinetics

Isothermal calorimetry [15] was used to establish the rates of HAp formation in deionized water and in 17 mM, 50 mM, and 150 mM acetic acid and citric acid solutions at 38°C using a liquid:solids weight ratio of 1. The rates of heat evolution were determined at a constant temperature by separately equilibrating the liquid and solid reactions to 38°C. The liquid was contained in a syringe and the solid reactants in a gold plated copper calorimeter cup. The cup was sealed with "Parafilm" to minimize endothermic effects of water evaporation. Once thermal equilibration was achieved, the liquid was injected on the solid and reaction initiates. The calorimeter cup was in thermal contact with thermopiles which convert the heat output to a voltage output. In a typical experiment, 3 g of solid HAp precursors were used and the voltage outputs were determined at 1 min intervals and collected using a microprocessor. Using the appropriate thermoelectric coefficient curves the rate of heat evolution or the total heat evolved (integral of the rate curve) may be plotted against time.

### 2.4 Solution chemistry

The effects of two concentrations of citric acid (3.4 and 10 mM) and acetic acid (4 and 50 mM) on the variations in the aqueous phase during HAp formation were determined. HAp precursors (50 g) were added to 250 ml of solution equilibrated to 38°C in a double-

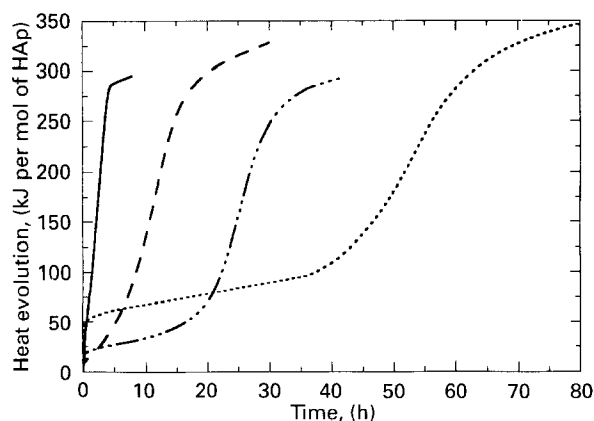


Figure 1 Heat evolution curves for HAp formed in deionized water (—), and 17 mM (---) and 50 mM (- · - · -), and 150 mM (···) citric acid solutions at 38°C.

walled beaker. Nitrogen gas was bubbled through the suspension throughout the reaction to minimize the presence of carbonates. A pH datum point was acquired by a microprocessor every minute using a combination glass electrode. Aliquots were extracted at selected times and filtered through 0.22  $\mu$ m disposable filters. The supernatants were analyzed for calcium and phosphate concentrations by DC plasma emission spectroscopy and for acetate and citrate concentrations by ion chromatography. Solids were extracted at selected times and quenched with acetone to stop further reaction. These were analysed by X-ray diffraction to determine the mineral phases present.

### 2.5. Infrared spectroscopy

Fourier transform infrared spectroscopy was performed over the wavenumber range 400–4000  $\text{cm}^{-1}$  using a Bomem single beam spectrometer with a resolution of 2  $\text{cm}^{-1}$ . The spectra of HAp formed in deionized water, citric acid, and acetic acid solution and that of calcium citrate and of a mixture (3 wt%) of calcium citrate and HAp were determined. Citrate was present in all citrate-HAp samples. All samples were dried in a vacuum oven at 120°C for 2 days. The KBr pellet technique was used.

## 3. Results and discussion

### 3.1. Kinetics

Figs 1 and 2 show the total heat evolved, in kJ per mol of HAp formed, during reaction in the citric and acetic acid solutions. These heat evolution curves indicate that the time required for complete reaction is greatly influenced both by the acid and its concentration. Times for complete reaction range from 3 h in 150 mM acetic acid to 75 h in 150 mM citric acid.

Fig 1 shows that heat evolution occurs in three stages of reaction. Each is influenced by the concentration of citric acid. Initially there is a short period of rapid heat evolution. Initial reaction involves the dissolution of TetCP and increases with increasing acid concentration. This can be seen by comparing the slopes of the heat evolution curves and the amounts of heat evolved during this period. As the concentration of citric acid is increased from 17 mM to 150 mM the heat evolved increases from 10 to 50 kJ per mol of

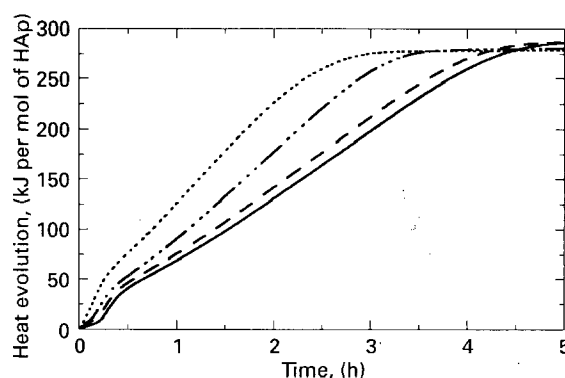


Figure 2 Heat evolution curves for HAp formed in deionized water (—), and 17 mM (---), 50 mM (- · - · -), and 150 mM (···) acetic acid solutions at 38°C.

HAp. Following this period of initial reaction is a period when heat evolution is low. The duration of this period increases with increasing citric acid concentration. The majority of heat evolution occurs in the final period of reaction and this is when the majority of HAp forms. Until the consumption of reactants approaches completion, the heat evolution during this final period occurs at a constant rate. These rates are proportional to the concentration of citric acid, decreasing with increasing acid concentration.

Unlike citric acid, acetic acid accelerates the formation of HAp (Fig. 2). HAp formation reaches completion in less than 3 h in the highest concentration of acetic acid studied. Reaction in acetic acid solution occurs in two stages. The first of these is dominated by dissolution of TetCP. The rates of reaction during this period increase with increasing acid concentration. However, the amount of heat evolved in this first stage does not exhibit a strong dependence on the concentration of acid. Reaction rates in the second stage of reaction also increase with increasing acetic acid concentration. The slopes of the linear portions of the curves in Figs 1 and 2 are related to the rates of HAp formation and are plotted as a function of acid concentration in Fig. 3. An increasing concentration of citric acid decreases the rate of HAp formation, and this decrease appears to be linear with concentration. Conversely, increasing the acetic acid concentration increases HAp formation at a rate which is also nominally linear. However, a maximum rate has not been reached in the range of concentrations studied.

### 3.2. Solution chemistry

#### 3.2.1. Citric acid

Fig. 4 shows the variations in citrate, calcium and phosphate concentrations depending on the initial concentration of citric acid. Regardless of the initial citric acid concentration, the calcium and citrate (when present) concentrations decrease with time. Citrate decreases to approximately half of the initial concentration within 30 min, Fig. 4a. Because the initial concentration of citrate is not high enough to precipitate its calcium salt, this decrease is associated

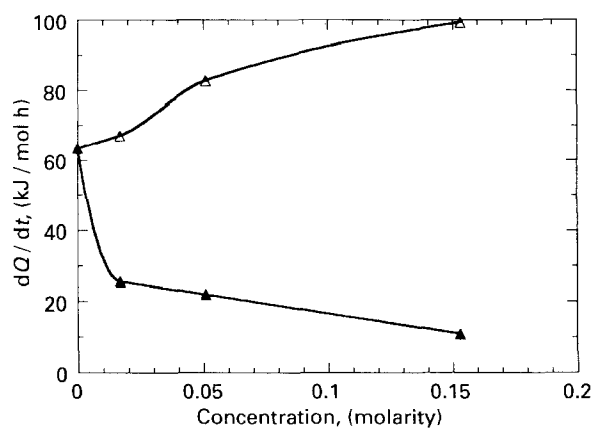
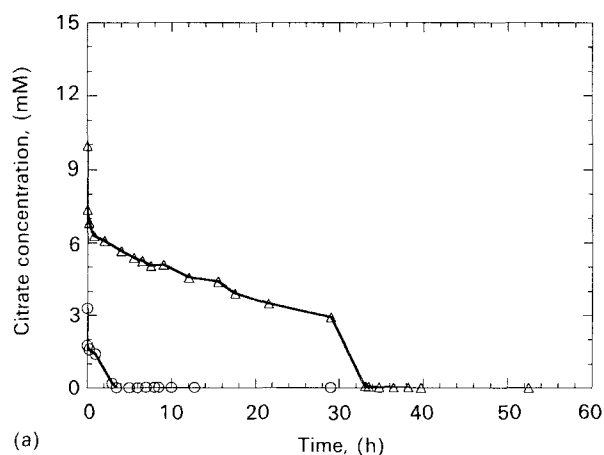
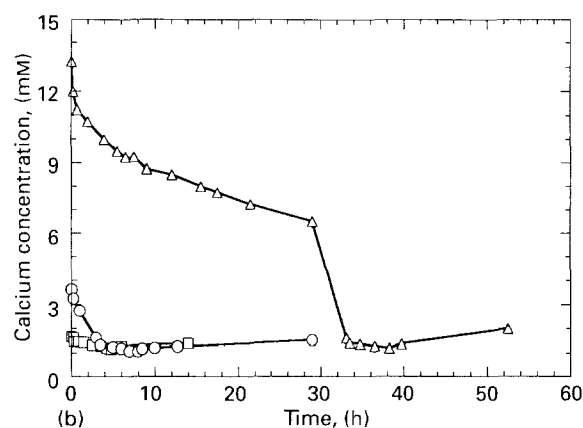


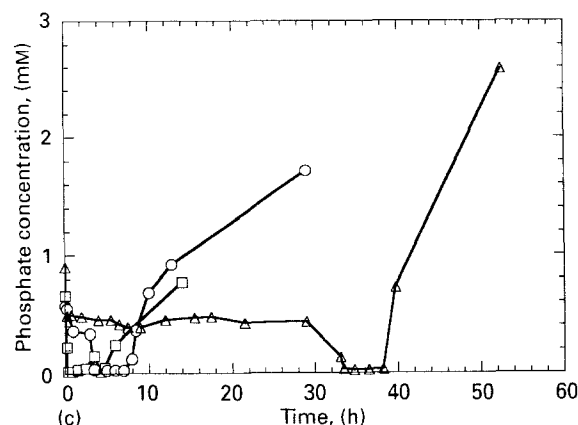
Figure 3 The rate of heat evolution ( $dQ/dt$ ) plotted as a function of acid type and concentration. These slopes were obtained from the linear period in Figs. 1 and 2 over which HAp formation occurs most rapidly;  $\Delta$  acetic;  $\blacktriangle$  citric.



(a)



(b)



(c)

Figure 4 Variations in (a) citrate, (b) calcium, and (c) phosphate concentrations during reactions in deionized water ( $-\square-$ ) and 3.4 mM ( $-\circ-$ ) and 10 mM ( $-\Delta-$ ) citric acid solutions at 38 °C.

with the adsorption of citrate onto the reactant surfaces. This observation is in accord with the findings of previous investigators [5, 9] who noted that citrate adsorbs onto a variety of calcium phosphates.

The maximum values in the calcium concentrations occur immediately after mixing, Fig. 4b. The value of the maximum increases with increasing citric acid concentration. This maximum is the result of two factors. The first is that the solubilities of the calcium phosphate reactants are higher at lower pH values [1]. Second, elevated calcium concentrations are a result of the ability of citrate to strongly complex divalent cations [9]. The DC plasma method determines total calcium in solution regardless of whether it is present as free cations or complexed. The increase in calcium

concentration with citrate concentration also correlates with the increase in TetCP dissolution indicated by the changes in both rate and extent of heat evolution during the initial stage of reaction as shown in

Comparing Fig. 4a and b shows that the rates of change in the calcium and citrate concentrations are in correspondence. Both decrease sharply within the first few minutes after mixing and then decrease more slowly. When the initial concentration is 10 mM, the citrate concentration drops rapidly to  $\sim 6$  mM, then to  $\sim 3$  mM over 30 h and finally to  $\sim 0$  mM between 30 and 33 h. The calcium concentration drops from  $\sim 6.5$  mM to  $\sim 1.5$  mM during this latter period. Consistent with the manner in which heat evolution occurs, these changes are suggestive of the onset of rapid HAp formation after a lengthy induction period.

Changes in phosphate concentration are shown in Fig. 4c. Although the magnitudes of these variations are much smaller than those in calcium and citrate, they are in correspondence. When HAp is formed in deionized water, the phosphate concentration rapidly decreases to a value of  $\sim 0.02$  mM, where it remains until the reaction has reached completion. The phosphate concentrations in the citric acid solutions decrease from their initial values to a steady-state value of  $\sim 0.3$  mM. These steady-states are maintained until the citrate concentrations decrease to zero. When this occurs, the phosphate concentration decreases to a low value, nominally  $\sim 0.02$  mM, supporting a rapid precipitation process of HAp. The changes in solution concentrations also coincide with changes in pH and mineral phases as will subsequently be discussed.

As is typically observed [2, 16], the phosphate concentration rises as complete reaction is approached. Although the variations in solution chemistry were not monitored to a point where the final equilibrium was reached, experimental trends suggest that the final concentration of phosphate increases with increasing citrate molarity. This suggests, in turn, the possibility of partial citrate substitution for phosphate in HAp. Citrate substitution for surface phosphate groups in HAp has been proposed previously [6, 10]. The increase of phosphate in solution is not due solely to an increase in the overall solubility of HAp. Although the final calcium concentration appears to increase slightly with an increase in the concentration of citric acid, the Ca/P ratio in solution decreases from 1.9 to 0.73 with increasing citrate concentration. This finding supports the view that citrate partially substitutes for phosphate in HAp. However, such substitution is primarily confined to the surfaces of the HAp crystallites because the citrate molecule is too large to be incorporated into the apatite structure [6].

The adsorption of citrate is consistent with the microstructure developed. Hollow shells of HAp are prevalent when reaction occurs in the presence of citrate, Fig. 5. This suggests that the dissolution of the reactants is retarded by a surface phenomenon. Because an initial acid-base reaction occurs between TetCP and citric acid, it is likely that these shells are TetCP relicts. Blockage of dissolution sites leads to the extended periods of slow reaction observed in Fig. 1.



Figure 5 Microstructure of HAp formed in a 150 mM citric acid solution at 38 °C showing the small needle dimensions and hollow shells resulting from citrate adsorption.



Figure 6 Microstructure of HAp formed in deionized water at 38 °C. Note the larger needle dimensions as compared to those in Figure 5.

Only when citrate is exhausted from solution does the rate of dissolution of the reactants accelerate. Eventually TetCP dissolution is complete leaving these hollow shells.

The microstructure of HAp formed in deionized water is shown in Fig. 6. Compared with reaction in water, the size of the HAp needles are reduced when reaction occurs in citric acid. This suggests that the citrate may also adsorb onto the surfaces of HAp nuclei and inhibit their growth.

The variations in pH during HAp formation in the citric acid solutions were monitored simultaneously with those in the ion concentrations and are shown in Fig. 7. Two steady-state pH values, one at pH  $\sim 7.3$  and another at pH  $\sim 8.5$  are observed in all experiments. The first steady-state occurs when DCP, TetCP, and minor amounts of DCPD are present. This steady-state pH is very close to that of the invariant point between TetCP and DCPD [1]. X-ray diffraction analyses show that DCPD forms upon initial mixing. DCPD is formed regardless of whether reaction occurs in water or in the acid solutions. Therefore, DCPD formation cannot be solely attributed to the reaction of TetCP with the acids. Rather DCPD formation appears to be related

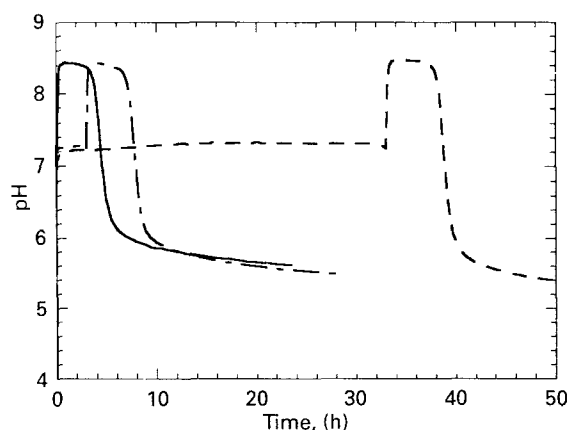


Figure 7 Variations in solution pH during reactions in deionized water (—) and 3.4 mM (---) and 10 mM (- · -) citric acid solutions at 38 °C.

to the presence of small amounts of an amorphous calcium phosphate formed during milling. When mixed with water, this amorphous calcium phosphate appears to immediately recrystallize forming DCPD. In spite of being present in a small proportion, DCPD controls the solution pH during the initial reaction in all the experiments. This steady-state pH is retained only for a few minutes when reaction occurs in deionized water. When citrate ions are not present to adsorb to the reactant surfaces, the small quantity of DCPD present reacts rapidly with TetCP and is consumed within the first 10 min of reaction. Only when DCPD has been consumed does the pH rise to a second steady-state pH near 8.5. Reactions in citric acid solution also result in this first steady-state pH. The length of time during which a steady-state pH near 7.3 is maintained is proportional to the initial concentration of citrate in solution and results from the adsorption of citrate on the reactant and product phases.

Comparison between Fig. 4 and 7 shows that the pH increases to 8.5, commensurate with the decrease in citrate concentration to zero, and the calcium and phosphorus concentrations to  $\sim 1.5$  mM and  $\sim 0.02$  mM, respectively. This suggests that little reaction occurs until the dissolution of the reactants is no longer limited by surface adsorption of citrates. However, based on heat evolution during these periods, HAp formation is slowly occurring and likely involves reaction of both DCP and DCPD with TetCP. Regardless of the presence and concentration of citrate, at the consumption of DCPD the pH increases to a value of 8.5. Thus, it would appear that the first steady-state pH is associated with the invariant point between DCPD and TetCP. The pH value of the second steady-state is higher than 7.7, which is the pH of the invariant point between DCP and TetCP [1]. Thus, the reaction at this steady-state is limited by the dissolution of DCP.

X-ray diffraction shows that HAp formation is greatest at this second steady-state condition. X-ray diffraction analysis also indicates that the disappearance of TetCP precedes that of DCP in every instance; associated with this is a decrease in pH to a constant value near 5.5. TetCP is consumed after 4.5, 7.5 and

38 h, for reactions in deionized water, 3.4 mM citric acid, and 10 mM citric acid, respectively. The formation of HAp at a pH of 8.5 and the disappearance of TetCP before that of the DCP indicates that the HAp formed initially has a Ca/P ratio greater than 1.5 [2]. Because the reactants were mixed in the proportion to produce HAp having a Ca/P of 1.5, the remaining DCP reacts with the previously formed HAp resulting in its compositional adjustment to a Ca/P of 1.5. As this occurs, the pH eventually drops to a value of  $\sim 5.5$  in all instances. Assumption of a Ca/P = 1.5 at complete reaction ignores the possibility of citrate substitution for phosphate. However, no discernable differences in the diffraction patterns of the HAp formed upon complete reaction were observed regardless of the presence of citric or acetic acids.

### 3.2.2. Acetic acid

The changes in calcium and acetate (when present) concentrations when HAp forms in various acetic acid solutions are shown in Fig. 8. The initial calcium concentrations increase with increasing acid concentration from 1.7 mM in deionized water to 25 mM in 50 mM acetic acid. As Fig. 2 shows, acetic acid enhances the initial dissolution of TetCP by lowering of pH. This results in an increased rate of early reaction as shown by heat evolution. When reaction occurs in deionized water and the 4 mM acetic acid solution, the calcium ion concentrations decrease only slightly to values of 1.2 mM and 2.2 mM, respectively; the acetate concentration does not change. Reaction in the more concentrated acetic acid solution results in a much larger change in the calcium concentration. The high initial value is again associated with a lower pH and increased solubility. The calcium concentration continuously decreases due to the formation of HAp. Upon complete reaction the calcium attains a value of 15–16 mM. A decrease in the acetate concentration is observed in the 50 mM acetic acid solution. However, this is followed by an increase in the acetate concentration to its original value. This suggests that acetate ion is adsorbed but eventually becomes desorbed at higher initial concentrations of acetic acid. The acetate concentration is at a minimum after about 3 h; based on X-ray diffraction analyses this is when the reaction has reached completion. The acetate concentration increases between 3 and 4.5 h after which time there are no further changes in solution.

Fig. 8c shows the variations in phosphate concentrations during HAp formation in deionized water and the acetic acid solutions. The phosphate concentrations decrease to a value of  $\sim 0.02$  mM where it remains until the reaction has reached completion. This is similar to the variations in phosphate observed in citric acid solutions. As in citric acid solution, the phosphate concentrations increase upon complete reaction and experimental trends suggest that their final concentrations will increase with increasing acetic acid concentration. Alternatively, in the acetic acid solutions, increasing acid molarity results in a significant increase in the final calcium concentration.

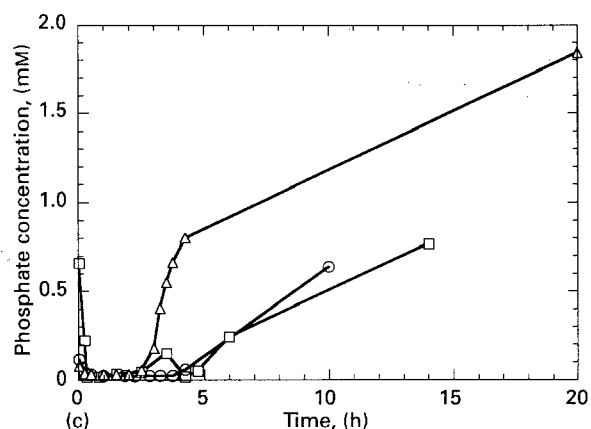
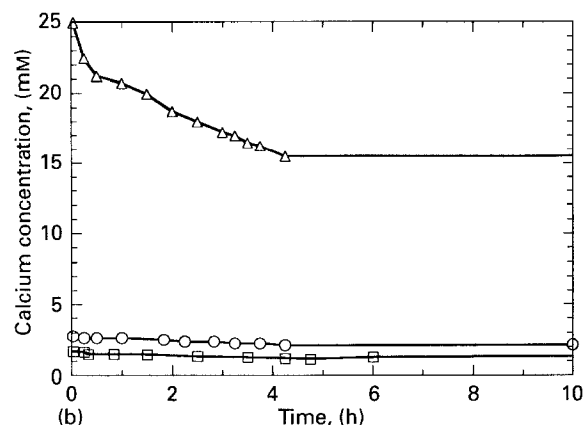
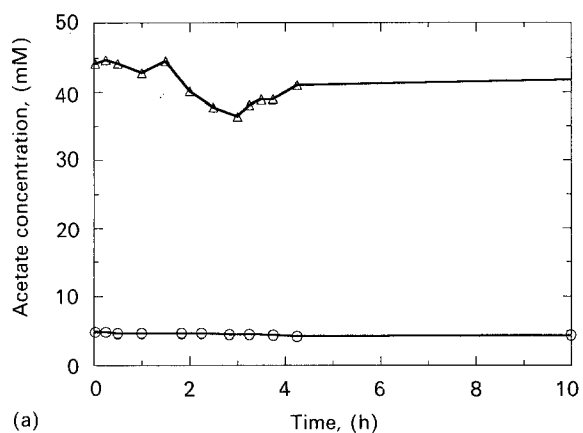


Figure 8 Variations in (a) acetate, (b) calcium and (c) phosphate concentrations during reactions in deionized water ( $\square$ ) and 4 mM ( $\circ$ ) and 50 mM ( $\triangle$ ) citric acid solutions at 38 °C.

Fig. 9. shows the pH variations in the acetic acid solutions and deionized water. Again, two steady-state pH values are observed. However, the time of the steady pH associated with the invariant point between DCPD and TetCP is of short duration. In addition, the values at these steady-state show a systematic decrease with increasing acetic acid concentration. The first steady-state value ranges between 6.8 and 7.3 while the second ranges between 7.8 and 8.5. This was not the case in the citric acid solutions. However, as observed in citric acid solutions, the disappearance of DCPD is again associated with the sharp increase in pH to the second steady-state pH. This is due to the same mechanism in both instances. Such a pH dependence is in accord with the results showing that

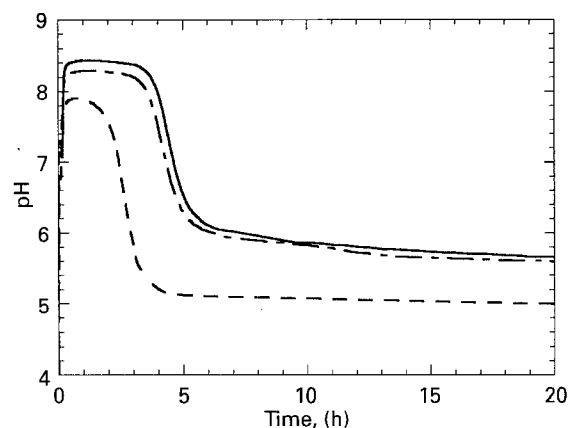


Figure 9 Variations in solution pH during reactions in deionized water ( $\text{—}$ ) and 4 mM ( $\text{-- --}$ ) and 50 mM ( $\text{- · -}$ ) acetic acid solutions at 38 °C.

both heat evolution and calcium concentration increase with increasing acetic acid concentration. These findings indicate that the acceleratory effect is essentially a pH phenomenon. In the absence of extensive adsorption, the reaction rate will increase with increased solubility of the reactant phases.

X-ray diffraction shows that HAP formation is extensive during this second steady state. As in citric acid solution, the disappearance of TetCP precedes that of DCP and again causes a drop in pH as the remaining DCP reacts with the HAP already formed to produce a final product with a Ca/P = 1.5. However, in acetic acid solutions the final pH values differ depending on the concentration of acetic acid. As shown in Fig. 9, the pH at complete reaction decreases to a value of 5 in the higher concentration of acetic acid, while it decreases to a value of  $\sim 5.5$  for the reaction in deionized water. Thus, the effects of acetic acid on HAP formation appear to be related solely to pH, while those of citric acid are related to the presence and binding affinity of the tricarboxyl citrate ion. The final pH value does not depend on the citric acid concentration because it decreases to zero. This indicates that citric acid is either adsorbed onto the surfaces of the HAP or becomes incorporated into it. This was further investigated by FTIR spectroscopy.

### 3.3. FTIR spectroscopy and surface area determinations

FTIR spectroscopy was carried out on the HAP formed in deionized water and in 50 mM acetic acid and 150 mM citric acid solutions during the calorimetric experiments. The HAP formed with citrate present will contain 3 wt% citrate assuming 100% incorporation. Therefore, spectra of calcium citrate and a mixture of calcium citrate with HAP (resulting in 3 wt% citrate with respect to the HAP) formed in deionized water were also obtained. Fig. 10 shows the carboxyl stretching region of calcium citrate, a mechanical mixture of HAP + calcium citrate, and HAP formed in citric acid (designated CtHAP). There are no significant differences between the spectra of calcium citrate and that in the calcium citrate + HAP mixture. Conversely, the number of carboxyl absorption bands and their

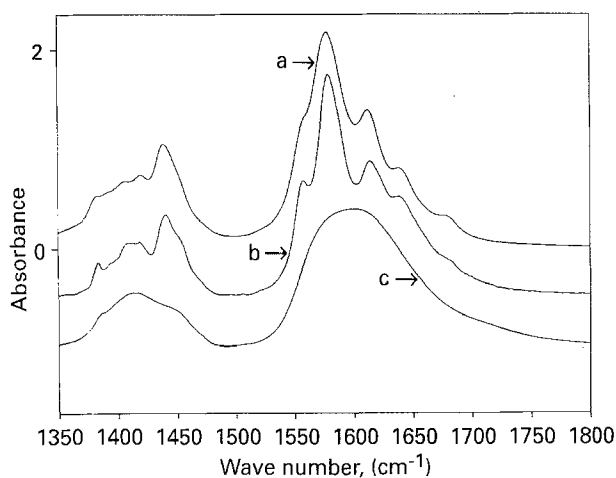


Figure 10 The carboxyl stretching region of the citrate molecule is shown. From top to bottom the spectra are those of (a) calcium citrate, (b) calcium citrate + HAp, and (c) HAp formed in a 150 mM citric acid solution.

shapes are modified in CtHAp when compared to those of calcium citrate. Similar results were observed by Cifuentes *et al.* [6]. In the present work the concentration of citric acid was below the solubility of calcium citrate, and no calcium citrate diffraction peaks were observed in X-ray studies. These results suggest an HAp–citrate association. Further evidence for such an association is presented in Fig. 11. This figure shows the stretching and bending modes of the phosphate tetrahedra. It is clearly evident that the stretching modes of the phosphate ion in the 1000–1200  $\text{cm}^{-1}$  region are both broader and less defined in CtHAp than in HAp. Such peak broadening and reduction in spectral features are indicative of increasing structural disorder and stress. Environmental effects such as these are caused by molecular interactions in the range of a few nanometers. These results, and the solution chemistry data showing increases in phosphorus concentration with citric acid molarity, indicate citrate substitution for phosphate in the apatite structure. However, TEM observations indicate that many of the HAp needles are comprised of crystallites 5–10 nm in width. These sizes are small enough for surface citrate adsorption to result in the spectral differences observed, namely peak broadening and reduction in structural features.

The BET surface areas of CtHAp, HAp formed in deionized water, and that formed in acetic acid are 117, 93, and 72  $\text{m}^2\text{g}^{-1}$ , respectively. These results support the view that citrate adsorbs onto HAp nuclei, inhibits their growth and resulting in the formation of a larger number of HAp crystallites which contribute a higher surface area. The small size of HAp crystallites makes it difficult to determine definitively whether citrate incorporation is purely an adsorption phenomenon or if some substitution occurs. While adsorption is supported substantially by the results of this study, we believe that there is also limited citrate substitution for phosphate on the surfaces of the apatite because, as previously reported [10], the phosphate concentration in solution increases with increasing acid concentration.

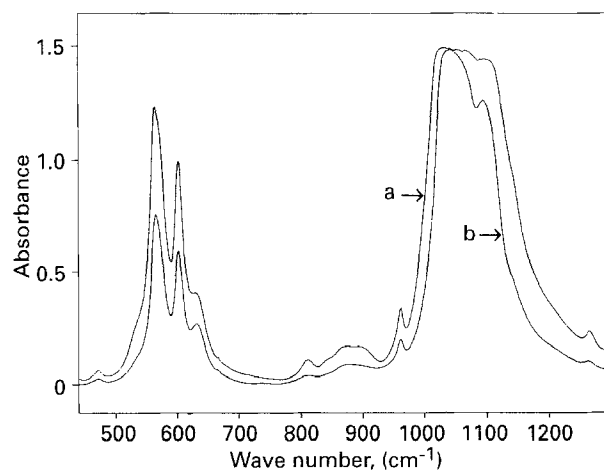


Figure 11 The stretching and bending modes of the phosphate group in HAp is shown. The spectra are those of HAp (a) formed in 150 mM citric acid and (b) that of calcium citrate + HAp.

#### 4. Summary

It is important to be able to control both the rate and conditions if HAp-based biomaterials, which form *in vivo*, are to be developed. Formation of HAp is affected by acetic and citric acids. The time to complete HAp formation is a strong function of both the concentration and type of acid present. The acceleratory effect of acetic acid is due to increased solubilities of the reactant phases at lower pH. Conversely, retardation by citric acid is related to the complexing and adsorbing ability of the tricarboxylate citrate molecule. Three periods of reaction are observed in isothermal calorimetry for reactions in citric acid. The first period is associated with the dissolution of TetCP, subsequent complexation of citrate with calcium ions which enter solution, and with adsorption of citrate onto the surfaces of the reactants. The second stage is due to the slow reaction of TetCP with DCPD and DCP. A steady-state pH occurs during this period. After DCPD has been consumed, the final period of reaction, associated with a second steady-state pH, occurs during the reaction between DCP and TetCP. Microstructural observation and solution chemistry data support the view that citrate adsorb onto both the reactant and product phases. Solution chemistry results also suggest partial substitution of citrate for phosphate. Changes in both the carboxyl and phosphate spectral features indicate a perturbation due to a HAp–citrate association. Due to the crystallite size of the HAp, these observations could be due to citrate substitution and/or adsorption.

#### Acknowledgements

The support of the National Science Foundation Bioengineering and Environmental Systems Section, grant BCS-8908631, is gratefully acknowledged. The authors would like to thank professor David Allara, Department of Materials and Chemistry, The Pennsylvania State University, for the use of his FTIR spectrometer.

#### References

1. W. E. BROWN (ed) and L. C. CHOW, in "Cements Research Progress 1986", (1987) p. 353.

2. P. W. BROWN and M. T. FULMER, *J. Amer. Ceram. Soc.* **74** (1991) 934.
3. P. W. BROWN, N. HOCKER and S. HOYLE, *ibid.* **74** (1991) 1848.
4. M. T. FULMER, R. MARTIN and P. W. BROWN, *J. Mater. Sci.: Mater. Med.* **3** (1992) 299.
5. Lj. BRECEVIC and H. FUREDI-MILHOFER, *Calcif. Tissue Int.* **28** (1979) 131.
6. I. CIFUENTES, P. F. GONZALEZ-DIAZ and L. CIFUENTES-DELATTE, *ibid.* **31** (1980) 147.
7. M. KNUUTTILA, R. LAPPALAINEN, P. ALAKUIJALA, and S. LAMMI, *ibid.* **37** (1985) 363.
8. M. KNUUTTILA, M. SVANBERG and M. HAMALAINEN, *Bone and Mineral* **6** (1989) 25.
9. H. M. MYERS, *Calcif. Tissue Int.* **40** (1987) 344.
10. C. Y. C. PAK and E. C. DILLER, *ibid.* **4** (1969) 69.
11. J. D. TERMINE and A. S. POSNER, *Arch. Biochem. Biophys.* **140** (1970) 307.
12. W. C. THOMAS, *Proc. Soc. Exper. Biol. Med.* **170** (1982) 321.
13. C. HOLT, M. J. M. VAN KEMENADE, L. S. NELSON, Jr., D. W. L. HUKINS, R. T. BAILEY, J. E. HARRIES, S. S. HASAIN and P. L. De BRUYN, *Mater. Res. Bull.* **23** (1989) 55.
14. R. K. CANNAN and A. KIBRICK, *JACS* **60** (1938) 2314.
15. E. J. PROSEN, P. W. BROWN, F. L. DAVIES and G. FROHNSDORFF, *Cem. Concr. Res.* **15** (1985) 703.
16. K. S. TENHUISEN and P. W. BROWN, *J. Dent. Res.* (in press).

*Received 5 May 1992 and  
accepted 19 May 1993*